

Lead-free piezoelectric ceramics based on perovskite structures

T. Takenaka · H. Nagata · Y. Hiruma ·
Y. Yoshii · K. Matumoto

Received: 19 March 2006 / Accepted: 5 January 2007 / Published online: 24 February 2007
© Springer Science + Business Media, LLC 2007

Abstract The piezoelectric properties of a solid solution based on three components of bismuth sodium titanate ($\text{Bi}_{1/2}\text{Na}_{1/2}\text{TiO}_3$ (BNT), bismuth potassium titanate, ($\text{Bi}_{1/2}\text{K}_{1/2}\text{TiO}_3$ (BKT), and barium titanate, BaTiO_3 (BT), that is $x(\text{Bi}_{1/2}\text{Na}_{1/2})\text{TiO}_3-y(\text{Bi}_{1/2}\text{K}_{1/2})\text{TiO}_3-z\text{BaTiO}_3$, [$x+y+z=1$, abbreviated as $\text{BNBK}_y\text{z}(x)$] and potassium niobate, KNbO_3 (KN) based ceramics, that is $\text{KN}+\text{MnCO}_3x$ wt.%, [abbreviated as $\text{KN-Mn } x$], were studied as a lead-free piezoelectric material. In the case of $\text{BNBK}2:1$ system, high piezoelectric properties were obtained near the MPB composition, and the highest electromechanical coupling factor, k_{33} and piezoelectric constant, d_{33} , were 0.58 for $\text{BNBK}2:1(0.89)$ and 181 pC/N for $\text{BNBK}2:1(0.88)$. Nevertheless, the depolarization temperature, T_d , shifts to lower temperature around the MPB compositions, and the T_d 's of $\text{BNBK}2:1(0.88-0.90)$ are only about 100 °C. On the tetragonal side, the T_d shifts to higher temperature with increasing the lattice anisotropy, c/a . As T_d higher than 200 °C was obtained in the range of $x < 0.78$, with a k_{33} and d_{33} for $\text{BNBK}2:1(0.78)$ being 0.45 and 128 pC/N, respectively. In the case of Mn doped KN ceramics, dense and non deliquescence KN ceramic were successfully obtained via ordinary firing technique in air by optimizing the fabrication process. Mn doping for KN ceramics was effective to obtain full poling state easily under poling conditions of high temperature and high electric field. As a result, we obtained the excellent piezoelectric properties of $k_{33}=0.507$ for $\text{KN-Mn}0.2$.

Keywords Lead-free piezoelectric ceramics · Piezoelectric constant · Electromechanical coupling factor · Ferroelectric properties · Depolarization temperature

1 Introduction

The piezoelectric property plays an important role for electric materials. The most widely used piezoelectric materials are based on the $\text{PbTiO}_3\text{-PbZrO}_3$ system (PZT) [1, 2]. However, it is desired that lead-free materials be used for environmental protection. For example, the legislation will be enforced in the EU as the draft Directives on Waste from Electrical and Electronic Equipment (WEEE), Restriction of Hazardous Substances (RoHS) and End-of Life Vehicles (ELV) [3]. Therefore, lead-free piezoelectric materials have been attracting attention as new materials in place of PZT materials. To replace PZT systems, it is necessary to consider specific application such as actuators, ultrasonic, filter, transducer or resonators etc. For high power applications, perovskite type ceramics seem to be high potential materials to replace PZT ceramics. Candidate materials for lead-free piezoelectric ceramics with the structure are BaTiO_3 (BT), ($\text{Bi}_{1/2}\text{Na}_{1/2}\text{TiO}_3$ (BNT), ($\text{Bi}_{1/2}\text{K}_{1/2}\text{TiO}_3$ (BKT), and KNbO_3 (KN) etc.

BT, BNT and BKT are well known ferroelectrics with the perovskite structure. BT is expected to be one of the superior candidates for lead-free piezoelectrics, however, the Curie temperature, T_c , of BT is too low at 135 °C, limiting the working temperature range. BNT [4–6] also has high potential for lead-free piezoelectrics, however, the depolarization temperature, T_d , occurs at about 200 °C. BKT has a tetragonal symmetry at room temperature and relatively high T_c [7, 8]. However, this ceramic is difficult to fabricate in a dense body. To improve problems such as

T. Takenaka (✉) · H. Nagata · Y. Hiruma ·
Y. Yoshii · K. Matumoto
Department of Electrical Engineering,
Faculty of Science and Technology,
Tokyo University of Science, Noda 2641,
Chiba-ken 278-8510, Japan
e-mail: tadashi@takenaka.ee.noda.tus.ac.jp

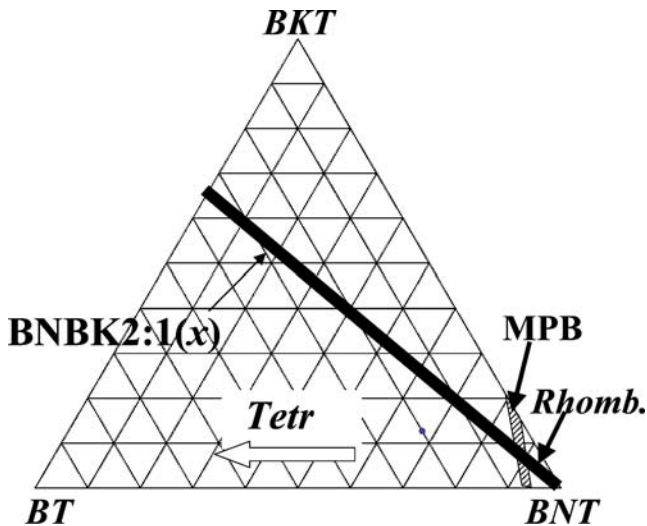


Fig. 1 Phase relationship of ternary system between $(\text{Bi}_{1/2}\text{Na}_{1/2})\text{TiO}_3$ (BNT), $(\text{Bi}_{1/2}\text{K}_{1/2})\text{TiO}_3$ (BKT) and BaTiO_3 (BT), where the bold solid line was investigated here as follows; $x(\text{Bi}_{1/2}\text{Na}_{1/2})\text{TiO}_3-y(\text{Bi}_{1/2}\text{K}_{1/2})\text{TiO}_3-z\text{BaTiO}_3$, [$x+y+z=1, y:z=2:1$, BNBK2:1(x);]

low T_c and inferior piezoelectric properties, binary systems of $\text{BaTiO}_3-(\text{Bi}_{1/2}\text{Na}_{1/2})\text{TiO}_3$, $(\text{Bi}_{1/2}\text{Na}_{1/2})\text{TiO}_3-(\text{Bi}_{1/2}\text{K}_{1/2})\text{TiO}_3$ and $\text{BaTiO}_3-(\text{Bi}_{1/2}\text{K}_{1/2})\text{TiO}_3$ solid solution systems have been reported [9–11]. Moreover, dielectric and piezoelectric properties of a solid solution based on three components of $\text{BaTiO}_3-(\text{Bi}_{1/2}\text{Na}_{1/2})\text{TiO}_3-(\text{Bi}_{1/2}\text{K}_{1/2})\text{TiO}_3$ near the morphotropic phase boundary (MPB) were recently investigated [12], and electromechanical coupling factor, k_{33} of 0.56 and piezoelectric constant, d_{33} , of 191 pC/N were obtained in 0.852BNT–0.120BKT–0.028BT. These values were relatively high among lead-free piezoelectric ceramics without grain orientation process, and the T_c near MPB was higher than 300 °C. Nevertheless, the

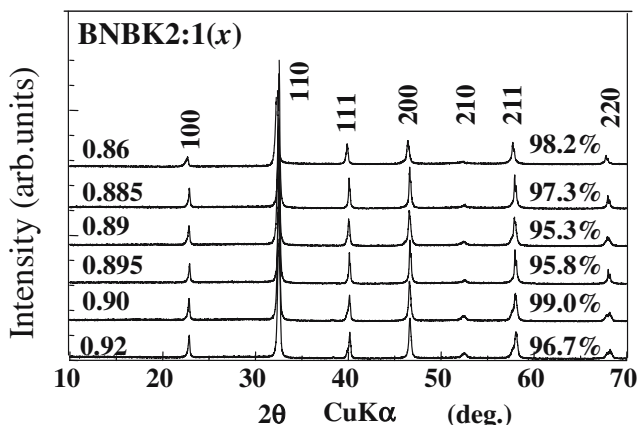


Fig. 2 X-ray diffraction patterns and density ratios of the ternary system, $x(\text{Bi}_{1/2}\text{Na}_{1/2})\text{TiO}_3-y(\text{Bi}_{1/2}\text{K}_{1/2})\text{TiO}_3-z\text{BaTiO}_3$, [$x+y+z=1, y:z=2:1$, BNBK2:1(x);]

depolarization temperatures, T_d , must be taken into consideration. In this paper, piezoelectric properties and the working temperatures (T_d) in the ternary system between BNT, BT, and BKT, shown in Fig. 1 are described as the first topic. Compositions on the bold solid line in Fig. 1 were investigated as follows.

1. $x(\text{Bi}_{1/2}\text{Na}_{1/2})\text{TiO}_3-y(\text{Bi}_{1/2}\text{K}_{1/2})\text{TiO}_3-z\text{BaTiO}_3$, [$x+y+z=1, y:z=2:1$, abbreviate as BNBK2:1(x);]

Figure 1 also shows the phase relationship between BNT, BT and BKT. This system has a MPB between rhombohedral (BNT) and tetragonal (BKT and BT) phase, respectively. In this study, compositions near the MPB were mainly investigated.

KNbO_3 (KN) is also well known lead-free piezoelectric material having a large piezoelectricity and high T_c [13–15], so that KN is picked up as the second topic in this paper. KN single crystal shows a large electromechanical coupling factor of the thickness-extensional mode, k_t , of 0.70 for the 49.5° rotated X -cut to the Y -axis, which is the highest among the present lead free piezoelectrics [14, 15]. However, in terms of KN ceramics, there are few papers and limited number of reports on electrical properties because of a deliquescence behavior and a poor sinterability of KN ceramics by conventional firing in air [16–21]. In this paper, we proposed a developed preparation procedure to improve the deliquescence and sinterability behavior of KN ceramics. Prepared compositions in this study are described as follows.

- (2) $\text{KNbO}_3+\text{MnCO}_3$ x wt.% [abbreviate as KN–Mn x]

KN–Mn x ceramics were basically prepared using the conventional ceramic fabrication process. To fix the problems of deliquescence and poor sinterability behavior, we optimized two conditions in whole sample preparation process. The first one is a calcination process for improvement of the deliquescence behavior, and the second one is a milling process for achieving fine KN powders and dense KN ceramic bodies.

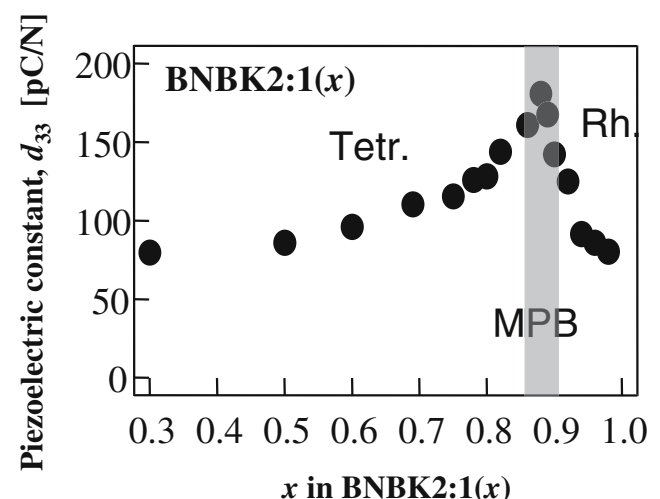


Fig. 3 Compositional dependence of the piezoelectric constant, d_{33} , for BNBK2:1(x)

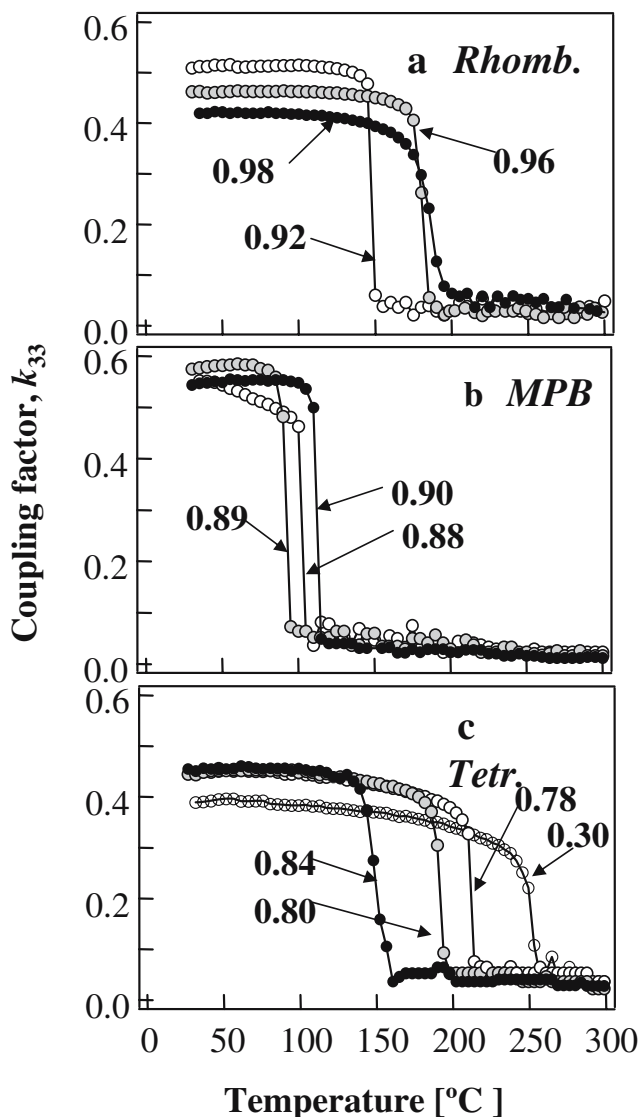


Fig. 4 Temperature dependence of electromechanical coupling factor, k_{33} , of **a** rhombohedral side of $x=0.92-0.98$, **b** MPB composition of $x=0.88-0.90$, **c** tetragonal side of $x=0.30-0.84$ in BNBK2:1(x)

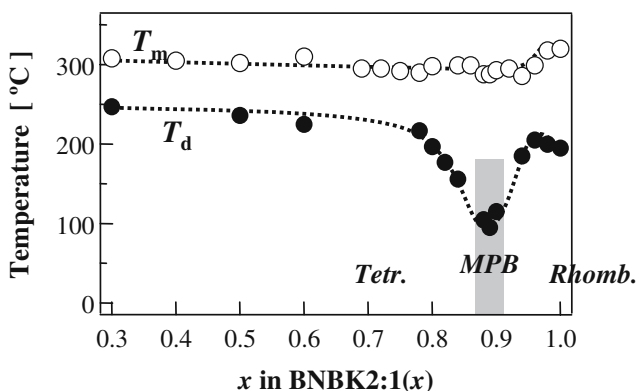


Fig. 5 Compositional dependence of the depolarization temperature, T_d and the temperature, T_m , determined by the maximum dielectric constant, ϵ_r , from the measurement of temperature dependence of ϵ_r .

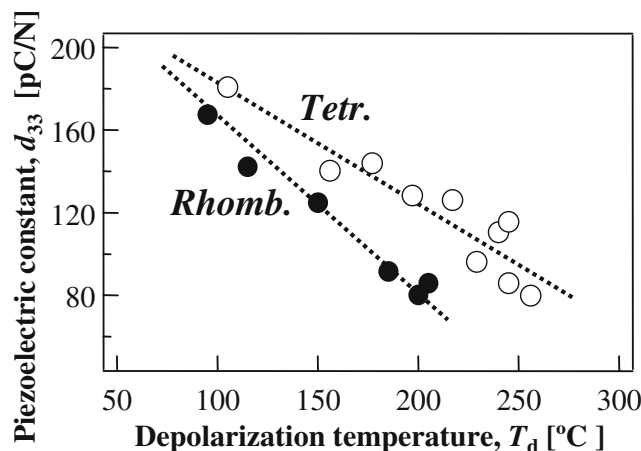


Fig. 6 The relationship between T_d and d_{33} of the tetragonal side and the rhombohedral side

2 Experimental procedure

Ceramic samples were prepared by using conventional sintering. Reagent-grade oxide powders of oxide and carbonate with 99+% purity were used as the starting materials. These materials were mixed by ball milling and calcined at 600–1,000 °C for 1–4 h. After calcining, the ground powders were ball-milled for 20 h and then pressed into discs of 20 mm diameter and 10 mm thickness by uniaxial pressing and subjected to a cold isostatic pressing (CIP) treatment at 150 MPa. These disks were sintered at 900–1,250 °C for 2–4 h in air. The crystal structure was confirmed by X-ray diffraction analysis using $\text{CuK}\alpha$ radiation at a scanning speed of 1 deg/min. Densities of obtained ceramics were measured using the Archimedes method. Samples were polished and thermally etched for microstructural examination by scanning electron microscopy (SEM, HITACH S-2400). The weight loss during the sintering process was analyzed by TG-DTA spectrometer (Rigaku, Thermo Plus 2).

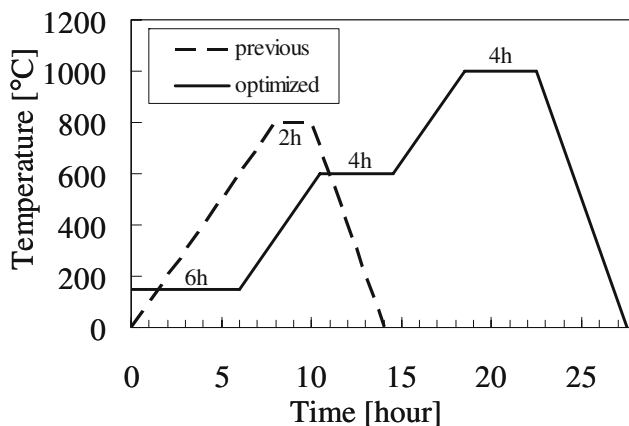
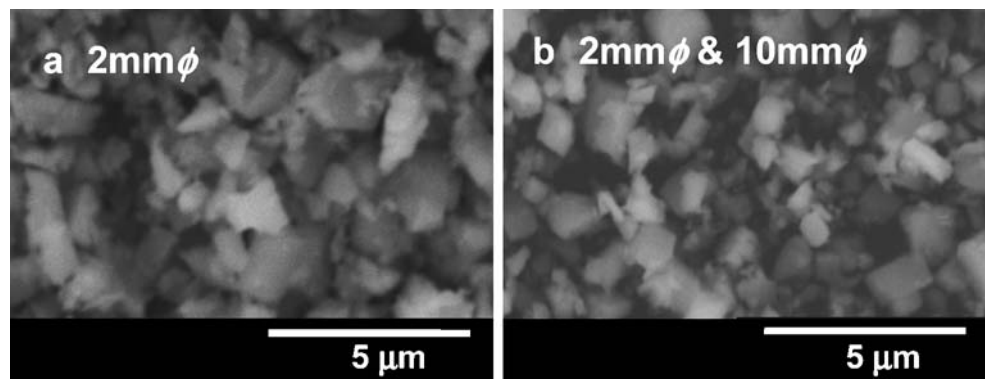


Fig. 7 Previous and optimized calcination pattern

Fig. 8 SEM micrographs of powder milled by **a** only 2 mm ϕ balls and **b** 2 and 10 mm ϕ balls, before sintering



Electrodes comprised of fired-on Ag–Pd paste were formed for electrical measurements, such as dielectric properties. The temperature dependence of dielectric constant, ϵ_s , and dielectric loss tangent, $\tan\delta$, were measured at 1 MHz using an automatic dielectric measurement system with a multifrequency LCR meter (HP 4275A) in the temperature range from RT to 500 °C. D – E hysteresis loops were observed using a virtual ground system (Toyo Corporation; Model 6252 Rev. C) at 50 Hz. Resistivity, ρ , was measured using a high-resistance meter (YHP 4329A and 4339B). The E-field strain behavior at room temperature was determined using a contact-type displacement sensor (Millitron; Model 1240) at 0.1 Hz.

Specimens for piezoelectric measurements were poled in stirred silicone oil at an applied field of $E_p=7$ –12 kV/mm, a temperature of $T_p=RT$ –200 °C, and a time of $t_p=7$ –10 min. Piezoelectric properties were measured by the resonance-antiresonance method on the basis of EMAS standards, using an impedance analyzer (YHP 4192A and 4194A). The longitudinal vibration of the (33)-mode was measured using a rectangular specimen of $4 \times 2 \times 2$ mm³. The electromechanical coupling factor, k_{33} , was calculated from the resonance and antiresonance frequencies. The free permittivity, ϵ_{ii}^T , was determined from the capacitance at 1 kHz of the poled specimens. The elastic constants, s_{jj}^E , were calculated from the frequency constant, N_{ij} , and the

measured density, ρ_0 . Finally, the piezoelectric constants, d_{ij} , were calculated from k_{ij} , ϵ_{ii}^T and s_{jj}^E . For example, the d_{33} was calculated from the following formula,

$$d_{33} = k_{33} \sqrt{\epsilon_{33}^T \cdot s_{33}^E}$$

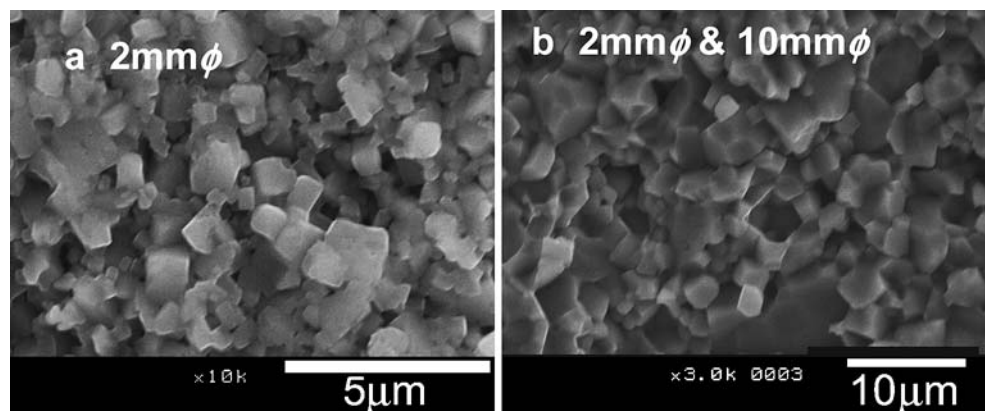
3 Results and discussion

3.1 $x(\text{Bi}_{1/2}\text{Na}_{1/2})\text{TiO}_3$ – $y(\text{Bi}_{1/2}\text{K}_{1/2})\text{TiO}_3$ – $z\text{BaTiO}_3$, [$x + y + z = 1$, $y:z=2:1$, abbreviate as BNBK2:1(x);]

The sintering temperatures shifted to lower temperatures and the sintering temperature range gradually became narrower with increasing ratio of BKT content, owing to the relatively low sintering temperature of BKT <1,060 °C. Figure 2 shows X-ray diffraction patterns and density ratios of BNBK2:1(x), [0.86–0.92]. The patterns for BNBK2:1 (0.3–0.98) show a single phase of perovskite structure with rhombohedral, tetragonal or complex rhombohedral and tetragonal symmetries, where the MPB exists in BNBK2:1 (0.89–0.90). The ceramics bodies were found to be more than 95% of the theoretical densities and were easily obtained in the BNBK2:1(0.3–0.98) system.

The compositional dependences of the piezoelectric coefficients, d_{33} , for BNBK2:1(x) are shown in Fig. 3.

Fig. 9 SEM micrographs of sintered KN ceramics milled by **a** only 2 mm ϕ balls and **b** 2 and 10 mm ϕ balls, before sintering



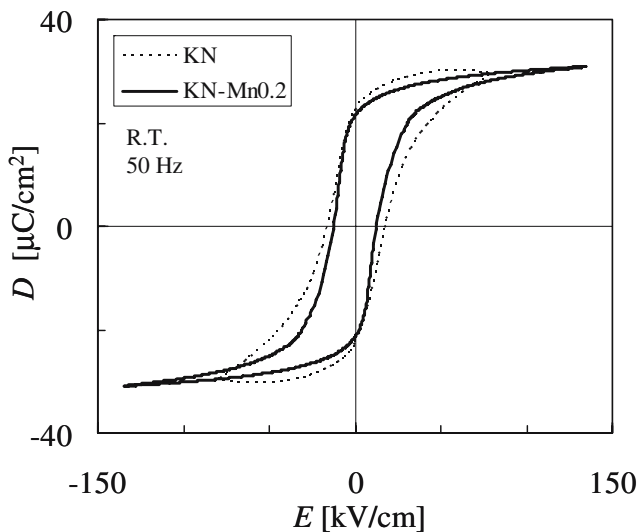


Fig. 10 D–E hysteresis loops of KN and KN–Mn0.2

High d_{33} values were obtained near the MPB composition being highest just on the tetragonal side. For BNBK2:1(x), d_{33} values >181 pC/N were obtained in BNBK2:1(0.88). On the tetragonal side, the d_{33} of BNBK2:1 decreased, as does both of k_{33} and ϵ_{33}^T . The d_{33} 's of BNBK2:1(0.98) and BNBK2:1(0.30) were found to be 80.3 and 79.9 pC/N, respectively.

It is important for BNT based solid solutions to investigate the actual working temperature for use in practical applications. For that reason, T_d was accurately determined from the depolarization temperature. The temperature dependences of k_{33} are shown in Fig. 4 for (a) rhombohedral side of $x=0.92$ – 0.98 , (b) MPB composition of $x=0.88$ – 0.90 , (c) tetragonal side of $x=0.30$ – 0.84 in BNBK2:1(x). It is recognized that the rhombohedral and tetragonal side exhibit a more stable k_{33} with temperature than for compositions around the MPB. The T_d and the temperature with maximum dielectric constant, T_m , of BNBK2:1(x) was summarized in Fig. 5. The T_m is determined by the temperature of the maximum dielectric

constant, ϵ_r , from the measurement of temperature dependence of ϵ_r . The T_m 's of BNBK2:1(x) were approximately the same as 300 °C, however, T_d was largely decreasing near the MPB composition, and T_d increased with decreasing the amount of BNT(x) content. It is thought these results indicate the T_d is dependent on lattice anisotropy (tetragonality), c/a . Figure 6 displays the relationship between T_d and d_{33} of the tetragonal side and the rhombohedral side. It is necessary for actual applications to obtain the value in the right upper corner (high d_{33} and high T_d) of this figure. However, the d_{33} and T_d indicated a trade-off relationship. The d_{33} as a function of T_d on the tetragonal side is higher than that on the rhombohedral side.

3.2 KNbO₃+MnCO₃ × wt.% [abbreviate as KN–Mn x]

Figure 7 shows previous and optimized calcination patterns. Before the calcinations, powders were pressed into pellets (30 mm diameter) with 80 MPa, after a drying of these pellets at 150 °C for 6 h. These pellets were heated with a rate of 100 °C/h till 600 °C and kept at that temperature for 4 h on the purpose for eliminating residual carbon and reacting potassium and niobium ions each other. Then it was heated till 1,000 °C and kept at that temperature for 4 h to be reacted completely. Cooling rate was 200 °C/h. After calcination, the ground powder was ball-milled for 24 h in ethanol with zirconia balls. In the milling process, two combinations of zirconia ball size were examined as (a) 2 mmϕ balls which is previous process and (b) 2 & 10 mmϕ balls which is new process in this study.

All of prepared samples were exposed to the water with ultrasonic vibrations. Any samples have no deliquescence. For this result, densities of obtained ceramics could be measured using Archimedes method. The dense ceramics bodies more than 95% of the relative densities to the theoretical densities were obtained. Obtaining dense KN ceramic by conventional method is basically difficult because potassium oxide (K₂O) is a volatile component

Fig. 11 Frequency dependence of impedance on the longitudinal (33)-mode for **a** KN and **b** KN–Mn0.2

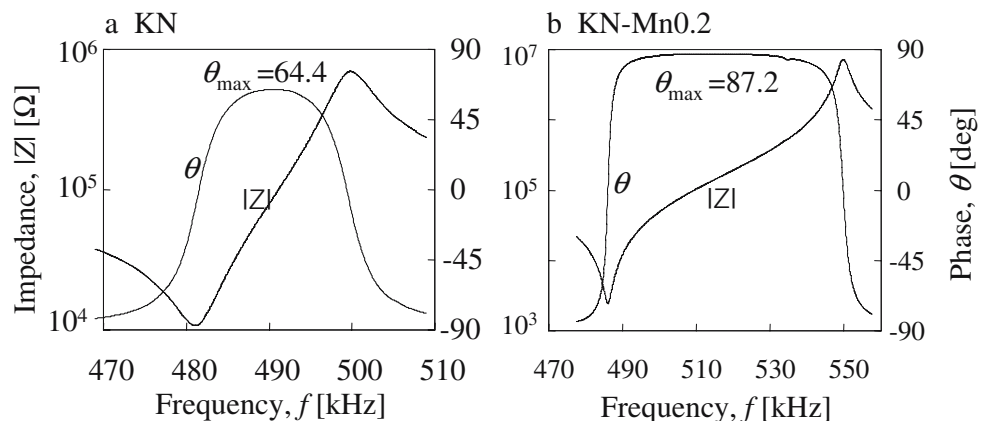


Table 1 Piezoelectric properties of KN systems based on several previous reports.

composition		k_p	k_t	k_{33}	d_{33} [pC/N]	Q_m	θ_{\max} [deg.]	method
KNbO ₃ -system	KNbO ₃ (this study)	–	–	–	0.295	66.4	106	OF
	KNbO ₃ +MnCO ₃ 0.2 wt.%, (this study)	–	–	0.507	85.7	282	87.2	OF
	KNbO ₃ +MnCO ₃ 0.8 wt.%, (this study)	–	–	0.43	71.5	482	87.3	OF
	KNbO ₃ [23]	0.25	0.18	–	–	–	–	OF(O ₂ rich atmosphere)
	KNbO ₃ +Bi ₂ O ₃ 0.5 wt.%+MnCO ₃ 0.3 wt.% [13]	–	–	0.31	89	–	70	OF
	96(KNbO ₃)–4{(Bi _{0.5} Na _{0.5})TiO ₃ } [24]	–	–	0.16	–	–	about –70	OF
	(K _{0.998} La _{0.002})(Nb _{0.998} Fe _{0.002})O ₃ [25]	0.17	–	–	*98	–	–	OF(K ₂ O rich atmosphere)
	(K _{0.998} La _{0.002})(Nb _{0.998} Fe _{0.002})O ₃ [26]	0.17	0.48	–	*98	–	–	OF(K ₂ O rich atmosphere)
	(K _{0.998} La _{0.002})(Nb _{0.998} Fe _{0.002})O ₃ +MnO ₂ 0.25 wt.%[26]	0.12	0.47	–	*90	–	–	OF(K ₂ O rich atmosphere)

* d_{33} meter value.

over 800 °C and evaporation from the system is accelerated by the humidity in the sintering environment [22]. This report indicates that K₂O is not a volatile component at 600 °C. Powders were calcined at 600 °C for 4 h as the first step in Fig. 7 to react each other and form a KNbO₃ structure without vaporization of potassium ions. We confirmed X-ray diffraction pattern of this samples showing single phase of perovskite structure. However, un-reacted potassium ions are still in the ceramics at this moment. The residual potassium ions act as key ions for absorbing humidity. That means this KN ceramic still has a problem of deliquescence. To solve this problem, these pellets were calcined at 1,000 °C for 4 h as the second step to react residual K ions completely with Nb ions. At the same time, the two step calcination process has a good advantage for preventing the vaporization of K ions during the second stage calcination at 1,000 °C because of the existence of the first step calcination at 600 °C. From the TG analysis, we did not see any weight losses of K ions in the same soaking pattern (600 °C and 1,000 °C) of two step calcination process in this experiment.

The sintering temperatures shift to lower temperature and available sintering temperature range gradually becomes wider with increasing the amount of the MnCO₃ content. Figure 8 shows SEM micrographs of powders milled by (a) only 2 mmϕ balls and (b) 2 and 10 mmϕ

balls, before the sintering. The powders milled by 2 and 10 mmϕ balls shown in Fig. 8b showed fine particles as compared with Fig. 8a. This result brought that dense KN ceramic was obtained by ordinary sintering technique. The crystal structures of KN–Mn x ($x=0.0\sim 0.8$) were confirmed by the X-ray diffraction patterns showing the single phase of perovskite structure and orthorhombic peaks splitting in the all sintered samples. Figure 9 shows the microstructures of KN ceramics prepared by (a) only 2 mmϕ balls and (b) 2 and 10 mmϕ balls. The dense ceramics bodies more than 95% of density ratio were obtained for KN ceramics prepared by (b) process. Preparation of fine particle powder is the key point of obtaining dense KN ceramics which is also reported by Birol et al [23].

Figure 10 shows D – E hysteresis loops of KN and KN–Mn0.2 ceramics. Remanent polarization, P_r , and Coercive field, E_c , were 23 $\mu\text{C}/\text{cm}^2$ and 18 kV/cm for KN, 21 $\mu\text{C}/\text{cm}^2$ and 12 kV/cm for KN–Mn0.2, respectively. The shape of D – E hysteresis loop in the KN ceramic is leaky. On the other hand, well saturated loop was obtained for the KN–Mn0.2 ceramic under high electric field. This result indicates that Mn doping is effective to obtain high resistance specimens under high electric field.

Figure 11 shows the frequency dependences of impedance on the longitudinal (33)-mode for (a) KN and (b)KN–

Table 2 Physical, electrical and piezoelectric properties of KN, and KN–Mn x ($x=0.2\sim 0.8$).

Samples	Relative density[%]	Resistivity ρ [$\Omega\cdot\text{cm}$]	$\epsilon_{33}^T/\epsilon_0$	θ_{\max}	Q_e	k_{33} [%]	Q_m	N_{33} [Hz·m]	s_{33}^E [pm^2/N]	d_{33} [pC/N]	g_{33} [$\times 10^{-3}$ Vm/N]
KN	96.7	1.8×10^{12}	580	64.4	2.1	29.5	106	2499	9.8	66.4	13
KN–Mn0.2	95.7	1.1×10^{11}	321	87.2	20.3	50.7	282	2754	10.0	85.7	30
KN–Mn0.4	95.6	6.0×10^{13}	343	85.1	11.6	48.5	185	2748	9.8	83.7	28
KN–Mn0.6	95.5	1.8×10^{13}	313	87.3	21.2	44.7	455	2729	9.5	72.5	26
KN–Mn0.8	96.1	3.5×10^{12}	340	87.3	21.0	43.0	482	2742	9.2	71.5	24

Mn0.2 samples. Note that the resonance wave of Fig. 11a was far from full poling state. The poling state was judged by the maximum phase, θ_{\max} of impedance in the inductance region between resonance and anti-resonance frequency. The θ_{\max} shown in Fig. 11a was 64.4° which is small comparing with Mn-doped samples (b). Nevertheless we obtained $k_{33}=0.295$, $d_{33}=66.4$ pC/N in pure KN ceramic which was poled under 4 kV/mm at 120°C . On the other hand, the resonance wave of Fig. 11b shows the well saturate poling state in the KN–Mn0.2 ceramic. This poling treatment was carried out under 6 kV/mm at 150°C . As a result, $\theta_{\max}=87.2^\circ$ and the highest k_{33} of 0.507 were obtained for KN–Mn0.2. It is estimated that difference of poling state between KN and KN–Mn0.2 depends on resistivity under high temperature and high electric field. The shapes of D–E hysteresis loops of KN and KN–Mn0.2 in Fig. 10 also are supporting this speculation.

Table 1 shows piezoelectric properties of KN systems based on several previous reports. The compositional dependences of electromechanical coupling factor, k_{33} for KN–Mn x were shown in Table 2. The high k_{33} were obtained for Mn-doped compositions. In Mn-doped KN ceramics, the highest k_{33} value of 0.507 was obtained at KN–Mn0.2. In addition, high k_{33} value of 0.492 was obtained at KN–Mn0.8. On the other hand, d_{33} values were not so high in the other KN systems because free permittivities were about half of other KN systems. The d_{33} of KN, KN–Mn0.2 and KN–Mn0.8 are 66.4 pC/N, 85.7 pC/N and 84.2 pC/N, respectively. In contrast, mechanical quality factor Q_m were relatively higher than the other KN systems. The Q_m of KN, KN–Mn0.2 and KN–Mn0.8 are 106, 282 and 349, respectively. Q_m tended to increase with increasing the amount of Mn content.

4 Conclusions

Dielectric ferroelectric and piezoelectric properties of lead-free perovskite type ceramics were investigated as candidates for a new group of lead free piezoelectric materials to reduce environmental damage. In the case of ternary system, that is, $x(\text{Bi}_{1/2}\text{Na}_{1/2})\text{TiO}_3-y(\text{Bi}_{1/2}\text{K}_{1/2})\text{TiO}_3-z\text{BaTiO}_3$, [$x+y+z=1$, abbreviate as BNBK $y:z(x)$], high piezoelectric properties were obtained near the MPB composition, and the highest electromechanical coupling factor, k_{33} and piezoelectric constant, d_{33} , were 0.58 for BNBK2:1(0.89) and 181 pC/N for BNBK2:1(0.88). Nevertheless, the depolarization temperature, T_d , shifts to lower temperature around the MPB compositions, and T_d 's of BNBK2:1(0.88–0.90) are about 100°C . On the tetragonal side, the T_d shifts higher with increasing lattice anisotropy, *c/a*. T_d 's higher than 200°C were obtained in the range of $x < 0.78$, with the k_{33} 's and d_{33} 's volume for BNBK2:1 being 0.45 and

128 pC/N, respectively. This ternary system seems to be a high potential to clear the requirements and specifications for actuator applications such as large $d_{33} > 200$ pC/N and high $T_c > 200^\circ\text{C}$. In the case of Mn doped KN ceramics, dense and non deliquescence KN ceramic were successfully obtained via ordinary firing technique in air by optimizing the fabrication process. Excellent piezoelectric properties of $k_{33}=0.507$ was obtained for KN–Mn0.2. This optimization of the process for making dense KN ceramics will be able to apply the other lead-free systems including potassium ions.

Acknowledgements The Authors would like to thank TOHO TITANIUM CO., LTD. For providing pure titanium oxide powders with high purity. This work was partially supported by a Grant-in-Aid for Scientific Research (B) (No. 17360327) from the Japan Society for the Promotion of Science.

References

1. E. Sawaguchi, J. Phys. Soc. Jpn. **8**, 615 (1953)
2. T. Yamamoto, Jpn. J. Appl. Phys. **35** 5104 (1996)
3. M. Shimada, Bulletin of the ceramic. Society of Japan **37**(11), 866 (2002)
4. G.A. Smolensky, V.A. Isupov, A.I. Agranovskaya, N.N. Krainic, Sov. Phys., Solid State **2**, 2651 (1961)
5. G.O. Jones, J. Kreisel, V. Jennings, M.A. Geday, P.A. Thomas, A. M. Glazer, Acta Crystallogr., B **58**, 168 (2002)
6. H. Nagata, T. Shinya, Y. Hiruma, T. Takenaka, Ceram. Trans. **167**, 213 (2005)
7. C.F. Buhner, J. Chem. Phys. **36**, 798 (1962)
8. Y. Hiruma, R. Aoyagi, H. Nagata, T. Takenaka, Jpn. J. Appl. Phys. **44**(7A), 5040 (2005)
9. T. Takenaka, K. Maruyama, K. Sakata, Jpn. J. Appl. Phys. **30** Part 1 (9B), 2236 (1991)
10. A. Sasaki, T. Chiba, Y. Mamiya, E. Otsuki, Jpn. J. Appl. Phys. **38** Part 1 (9B), 5564 (1999)
11. Y. Hiruma, H. Nagata, T. Takenaka, J. Ceram. Soc Jpn, S. **112**(5), S1125 (2004)
12. H. Nagata, M. Yoshida, Y. Makiuchi, T. Takenaka, Jpn. J. of Appl. Phys. **42**(12), 7401 (2003)
13. G. Shirane, R. Newnham, R. Pepinsky, Phys. Rev. **96**, 581 (1954)
14. K. Nakamura, T. Tokiwa, Y. Kawamura, J. Appl. Phys. **91**, 9272 (2002)
15. S. Wada, A. Seike, T. Tsurumi, Jpn. J. Appl. Phys. **40**, 5690 (2001)
16. L. Egerton, D.M. Dillon, J. Am. Ceram. Soc. **42**, 438 (1959)
17. M. Uniyal, K. Singh, S. Bhatt, R.P. Pant, D.K. Suri, B.S. Semwal, Int. J. Pure Appl. Phys. **41**, 305 (2003)
18. P. Dubernet, J. Ravez, Ferroelectrics **211**, 51 (1998)
19. R.E. Jaeger, L. Egerton, J. Am. Ceram. Soc. **45**, 209 (1962)
20. K. Toda, S. Tokuoka, N. Ohtake, K. Uematsu, M. Sato, Trans. MRS-J **28**, 353 (2003)
21. T. Yoshida, Y. Hiruma, R. Aoyagi, H. Nagata, T. Takenaka, Key Eng. Mater. **301**, 19 (2006)
22. U. Flueckiger, H. Arend, J. Am. Ceram. Soc. **56**, 575 (1977)
23. H. Birol, D. Damjanovic, N. Setter, J. Am. Ceram. Soc. **88**(7), 1754 (2005)
24. H. Ishii, H. Nagata, T. Takenaka, Jpn. J. Appl. Phys. **40**, 5660 (2001)
25. K. Kakimoto, I. Masuda, H. Ohsato, Jpn. J. Appl. Phys. **42**, 6102 (2003)
26. K. Kakimoto, I. Masuda, H. Ohsato, Jpn. J. Appl. Phys. **43**, 6706 (2004)